The Electronic Structure of Closed Shell Metallocenes in the Ground State and in the Cationic Hole-States

Michael C. Böhm

Institut für Organische Chemie der Universität Heidelberg, West Germany

Z. Naturforsch. **37a**, 1193–1204 (1982); received May 27, 1982

The electronic structure of tne closed shell metallocenes bis(π-cyclopentadienyl)magnesium (**1**), bisbenzene chromium (**2**), ferrocene (**3**) and cyclopentadienyl benzene manganese (**4**) has been studied in the ground state as well as in the low-lying cationic states. The computational framework is a semiempirical INDO Hamiltonian, the theoretical framework for the investigation of the cationic hole-states is the Green's function method. The calculated ionization energies are compared with the photoelectron (PE) spectra of the four closed shell metallocenes. The interrelation between theoretically determined reorganization energies and the localization properties of the orbital wave functions or the nature of the transition metal center is analyzed. General rules concerning the validity of Koopman's theorem in transition metal complexes are formulated.

1. Introduction

Ferrocene was one of the first examples in the class of transition metal compounds where the nonvalidity of Koopmans' theorem [1] ($I^{K}_{v,j} = -\varepsilon_j$) for ionization events in the outer valence region had been demonstrated [2]. The sequence of the canonical molecular orbital energies in the electronic ground state differed from the sequence of the calculated ionization potentials derived in an ab initio ΔSCF framework. It has been shown that orbital relaxation for electron ejections out of strongly localized iron 3d orbitals is of significant importance. Correlation effects however are not taken into account in the ΔSCF approximation. The theoretical shortcomings of computational approaches based on the one-particle picture of the Hartree-Fock (HF) approximation have been demonstrated in a large number of ΔSCF ab initio studies [3–5]. The neglected correlation contributions were often so large that wrong sequences for the ionization processes have been predicted.

Relaxation and correlation effects in vertical ionization processes can be taken into account by means of the Green's function formalism. In the case of transition metal compounds this method has been employed in connection with ab initio Hamiltonians [6] and in combination with semiempirical LCAO methods for molecules that are beyond the computational capacity of large scale ab initio bases. In connection with semiempirical MO models the Green's function formalism had been applied both in the inner [7] and the outer valence region [8–11]. The outer valence studies cited in [8–11] were based on a recently developed CNDO/INDO Hamiltonian for transition metal compounds [12]. The method has been designed to reproduce the results of timeconsuming ab initio calculations and has been applied in a larger numbre of 3d complexes with different types of organic ligands (carbonyl derivatives, organic π systems, half sandwich compounds, chelate rings).

In the present contribution we want to study the electronic structure in the ground state and the outer valence region in the photoelectron (PE) spectra of ferrocene and of related closed shell metallocenes. The ionization energies are calculated by means of the Green's function approach. We have chosen bis(π-cylopentadienyl)magnesium (**1**) as a representative example of a closed shell metallocene with outer valence MO's that are prevailingly localized in the Cp rings. Three complexes with occupied 3d orbitals have been considered: bisbenzene chromium (**2**), ferrocene (**3**) and the mixed sandwich cyclopentadienyl benzene manganese (**4**). The PE spectra of these compounds have been measured by several groups (**1**: [13], **2**: [14–16], **3**: [13, 17, 18] and **4**: [16]). Within the series **1**–**4** only the PE spectra of **2** [14] and **3** [2, 19, 20] have been discussed on the basis of computational results (ΔSCF calculations), the PE data of **1** and **4** have

Reprint requests to Dr. M. C. Böhm, Institut für Organische Chemie der Universität Heidelberg, Im Neuenheimer Feld 270 D-6900 Heidelberg.

0340-4811 / 82 / 1000-1193 $ 01.30/0. — Please order a reprint rather than making your own copy.

been presented with experimentally derived assignments.

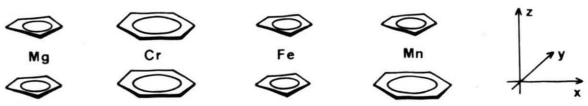

1 2 3 4

In the next section a short outline of the Green's function method is given. The ground state properties of **1**—**4** as derived in the present INDO model are discussed in chapter 3, the calculated ionization potentials in the lower energy region are presented in section 4. In the last paragraph general rules are derived that allow a rough assessment on the magnitude of reorganization energies in the PE spectra of transition metal complexes.

2. Computational Method

In the following only the most important aspects of the Green's function formalism are described. The method has been discussed in larger detail in our foregoing publications [8—11]. The interrelation between calculated Koopmans' defects and the parametrization of the semiempirical Hamiltonian has been analyzed for various transition metal complexes [21, 22]. The theoretical background of many-body perturbation theory and the capability of the formalism in combination with ab initio bases has been clarified in different contributions [23—25].

Ionization potentials in the Green's function approach are related to the zeros of the inverse Dyson equation (1) [26]

$$G^{-1} = (G^0)^{-1} - \Sigma(\omega) = \omega I - \varepsilon - \Sigma(\omega)\,. \quad (1)$$

G is the matrix of the Green's function, G^0 is the free Green's function associated to the diagonal canonical HF solution and ω is the energy coordinate that has to be determined. I symbolizes the unit matrix of proper size and ε is the (diagonal) matrix of the canonical MO energies. $\Sigma(\omega)$ is the socalled self-energy operator which can be expanded into a series (eq. (2)) according to different orders of perturbation.

$$\Sigma(\omega) = \Sigma^{(2)}(\omega) + \Sigma^{(3)}(\omega) + \cdots \Sigma^{(\infty)}(\omega)\,. \quad (2)$$

$\Sigma^{(1)}(\omega)$ vanishes in the case of canonical MO's and $\Sigma^{(2)}(\omega)$ is the leading term of the perturbational series. In accordance with our previous studies [10, 11, 21, 22] we have employed an effective renormalized self-energy approximation where the second order contributions of the $\Sigma(\omega)$ expansion are scaled by a single third order element (D4). The model potential of eq. (3) has been derived by Cederbaum on the basis of a geometric approximation [25].

$$\Sigma^{\text{eff}}(\omega) = \Sigma^{(2)}(\omega) + \text{D}4\,. \quad (3)$$

The nomenclature corresponds to [25]. The approximations used for the determination of the zeros in the inverse Dyson equation are the same than in our previous studies [9—11].

3. Ground State Properties

The electronic structure of the Mg complex **1** has not been analyzed on the basis of MO calculations. Various molecular orbital studies on the other hand have been carried out for the corresponding Be compound [27, 28]. In contrast to the Be derivative [29] it has been demonstrated by a gas-phase diffraction study that **1** is a symmetric sandwich compound with a negligibly small rotational barrier (0.8 kcal/mol) between the eclipsed D_{5h} and the staggered D_{5d} conformation [30].

The calculated orbital energies of **1** are summarized in Table 1. The irreducible representations correspond to the more familiar D_{5d} classification. The interrelation between the irreducible representations under D_{5d} and D_{5h} symmetry are displayed below:

D_{5d}	A_{1g}	A_{2g}	E_{1g}	E_{2g}	A_{1u}	A_{2u}	E_{1u}	E_{2u}
D_{5h}	A_1'	A_2'	E_1''	E_2'	A_1''	A_2''	E_1'	E_2''

The $4e_{1g}$ HOMO of **1** is the out-of-phase linear combination of the $e_1''(\pi)$ orbitals of the Cp ligands. The in-phase counterpart ($5e_{1u}$) is stabilized by Mg $3p_x/3p_y$ admixtures and is separated by 1.15 eV from the $4e_{1g}$ MO. The two highest degenerate orbitals show an energy gap of about 3 eV to the remaining Cp π and σ linear combinations. The net charge at the central atom amounts to 0.468, the carbon centers in the Cp moieties have a surplus of charge of -0.143 e.

The electronic structure of bisbenzene chromium has been investigated by different theoretical procedures: semiempirical LCAO models [31, 32], ab initio calculations in a near minimal basis [15] and statistical X_α approaches [33]. The INDO results for the high-lying valence orbitals are also

Table 1. Molecular orbitals of bis(π-cyclopentadienyl)manganese (**1**), bisbenzene chromium (**2**) and ferrocene (**3**) according to semiempirical INDO calculations. The MO wave functions have been decomposed into contributions from the central atom (Mg, Cr, Fe) and into ligand π and ligand σ admixtures (Cp = Cyclopentadienyl, Bz = Benzene).

Compound	MO	Γ_i	MO-Type	ε_i (eV)	% central atom	% ligand π	% ligand σ
1	25/26	$4e_{1g}$	Cp π	— 7.96		100.0	
	23/24	$5e_{1u}$	Cp π, Mg $3p_x/3p_y$	— 9.11	7.3	90.9	1.8
	21/22	$3e_{2u}$	Cp σ	— 12.23			100.0
	19/20	$4e_{1u}$	Cp σ	— 12.32	0.4		99.6
	18	$5a_{2u}$	Cp π	— 12.41	2.6	96.4	1.0
	16/17	$3e_{1g}$	Cp σ	— 13.06			100.0
	14/15	$3e_{2g}$	Cp σ	— 13.10			100.0
	13	$6a_{1g}$	Cp π, Mg 3s	— 15.66	13.0	80.1	6.9
2	33	$8a_{1g}$	Cr $3d_{z^2}$	— 8.52	95.0	0.1	4.9
	31/32	$4e_{2g}$	Cr $3d_{x^2-y^2}/3d_{xy}$	— 9.14	58.7	34.5	6.8
	29/30	$6e_{1u}$	Bz π	— 11.21	1.2	97.6	1.2
	27/28	$4e_{1g}$	Bz π, Cr $3d_{xz}/3d_{yz}$	— 11.25	14.2	67.2	18.6
	26	$6a_{2u}$	Bz π	— 11.71		99.1	0.9
	24/25	$3e_{2u}$	Bz σ	— 12.45			100.0
	22/23	$3e_{2g}$	Bz σ	— 12.82	4.8	0.4	94.8
3	28/29	$6e_{1u}$	Cp π	— 9.91	0.3	99.1	0.6
	27	$8a_{1g}$	Fe $3d_{z^2}$	— 10.75	93.4	2.7	3.9
	25/26	$4e_{1g}$	Cp π, Fe $3d_{xz}/3d_{yz}$	— 10.94	23.5	58.5	16.2
	23/24	$4e_{2g}$	Fe $3d_{x^2-y^2}/3d_{xy}$	— 11.22	90.1	6.1	3.8
	22	$6a_{2u}$	Cp π	— 11.62	0.3	99.2	0.5
	20/21	$5e_{1u}$	Cp σ	— 13.37			100.0
	18/19	$3e_{2u}$	Cp σ	— 14.03			100.0
	16/17	$3e_{1g}$	Cp σ, Fe $3d_{xz}/3d_{yz}$	— 14.04	14.5	5.1	80.4
	14/15	$3e_{2g}$	Cp σ	— 14.29	2.6		97.4
	13	$7a_{1g}$	Cp π	— 16.17	4.2	93.8	2.0

summarized in Table 1; the geometrical parameters have been adopted from the X-ray data of [34].

The two highest occupied MO's of **2** ($8a_{1g}$, $4e_{2g}$) are prevailingly localized at the 3d center; in analogy to the X_α model INDO predicts $8a_{1g}$ on top of $4e_{2g}$. The complex HOMO at — 8.52 eV has the largest 3d amplitude (95%) while the Cr 3d ligand coupling is enlarged in the degenerate $4e_{2g}$ combination. The 3d admixtures are reduced to 59%. The remaining occupied MO's of **2** are ligand-type functions. $6e_{1u}$ is the in-phase combination of the $1e_{1g}$ benzene HOMO. The corresponding out-of-phase function is stabilized by the Cr $3d_{xz}/3d_{yz}$ acceptors. As a result of the mutual compensation of "through-space" and "through-bond" interaction [35] a small energy gap ($\Delta\varepsilon = 0.04$ eV) between the degenerate $6e_{1u}/4e_{1g}$ MO pairs is predicted. The Cr 3d contributions in the remaining high-lying valence orbitals are small.

A large number of MO calculations with different degrees of sophistication have been performed on ferrocene [36—38]. A review of the literature shows that in most of the semiempirical approaches the iron 3d orbitals are predicted on top of the ligand functions while ab initio studies predict a ground state MO sequence with ligand π MO's above the Fe 3d functions. The INDO results on **3** (Table 1) are based on the experimental geometry [39]; the staggered D_{5d} conformation has been adopted for the calculations. The highest occupied MO of **3** in the electronic ground state is the in-phase linear combination of the degenerate e_1'' (π) orbitals of the cyclopentadienyl rings. The out-of-phase component, $4e_{1g}$, is stabilized via the Fe $3d_{xz}/3d_{yz}$ AO's and is separated by 1.03 eV from the $6e_{1u}$ HOMO. The two degenerate ligand functions are separated due to the $8a_{1g}$ ($3d_{z^2}$) MO. The iron admixtures amount to 93.4%. The localization properties of the orbital wave function are similar to the $8a_{1g}$ MO of the chromium complex. In contrast to **2**, however, also the $4e_{2g}$ combination ($3d_{x^2-y^2}/3d_{xy}$) is prevailingly localized at the transition metal center. The remaining MO's of **3** are ligand combinations (π and σ type) that form closely spaced in-phase and out-of-phase linear combinations. A large energy difference is only

Table 2. Molecular orbitals of cyclopentadienyl benzene manganese (**4**) according to the semiempirical INDO approach. The MO wave functions have been decomposed into Mn contributions and into admixtures (π and σ) from the Cp and Bz ligands. The irreducible representations in parenthesis correspond to the point group $C_{\infty v}$ (idealized model for **4**).

MO	Γ_i	MO-Type	ε_i (eV)	% Mn	% Cp π	% Cp σ	% Bz π	% Bz σ
31	29 a′ (a_1)	Mn 3 d_{z^2}	— 9.44	91.5	5.5	1.9	0.1	1.0
30	28 a′ (e_2)	Mn 3 $d_{x^2-y^2}$, Cp π, Bz π	— 9.77	63.5	22.1	1.3	11.0	2.1
29	22 a″ (e_2)	Mn 3 d_{xy}, Cp π, Bz π	— 9.77	75.9	8.1	1.0	12.5	2.5
28	27 a′ (e_1)	Cp π, Mn 3 d_{yz}/3 $d_{x^2-y^2}$, Bz π	— 9.78	28.6	61.6	1.2	6.8	1.8
27	21 a″ (e_1)	Cp π, Mn 3 d_{xz}/3 d_{xy}, Bz π	— 9.79	16.1	75.6	1.3	5.1	1.9
26	26 a′ (e_1)	Bz π, Mn 3 d_{yz}/3 $d_{x^2-y^2}$	— 11.47	8.1	0.3	10.6	79.2	1.8
25	20 a″ (e_1)	Bz π, Mn 3 d_{xz}/3 d_{xy}	— 11.47	8.2	0.4	10.1	79.5	1.8
24	25 a′ (a_1)	Cp π, Bz π, Mn 3 d_{z^2}	— 12.32	4.3	58.2	0.3	36.9	0.3
23	24 a′ (e_1)	Cp σ	— 12.99	4.8	0.4	85.6	5.5	3.7
22	19 a″ (e_1)	Cp σ	— 13.02	4.5	0.4	83.8	5.1	6.2
21	23 a′ (e_2)	Bz σ	— 13.13	1.6	0.0	1.7	0.0	96.7
20	18 a″ (e_2)	Bz σ	— 13.14	1.8	0.0	3.3	0.2	94.7
19	22 a′ (e_2)	Cp σ	— 13.58	0.8	0.0	98.0	0.1	1.1
18	17 a″ (e_2)	Cp σ	— 13.69	0.6	0.0	98.7	0.0	0.7

found in the case of the two π orbitals $6a_{2u}$ and $7a_{1g}$ ($\Delta\varepsilon \approx 4.5$ eV).

Cyclopentadienyl benzene manganese **4** is the remaining member in the isoelectronic series **2**→**3**→**4** and belongs to the class of mixed sandwich compounds that have been studied in large detail in the recent years [40—43]. As the X-ray structure of **4** is yet unknown we have extrapolated geometrical parameters from related organometallic manganese complexes [44].

The MO energies of **4** in the electronic ground state are summarized in Table 2, a graphical display of the outer valence orbitals is shown in Figure 1. The irreducible representations of **4** are labeled with respect to the point group C_s; additionally we have employed a classification scheme (in parenthesis) for Γ_i that is related to the point group $C_{\infty v}$ [45]. The 29a′ HOMO of **4** at — 9.44 eV is predominantly of Mn 3 d_{z^2} character with small antibonding a_2'' (π) admixtures from the Cp ring. 28a′ and 22a″ have a common e_2 parent (3 $d_{x^2-y^2}$/3 d_{xy} in $C_{\infty v}$). Both complex MO's show enlarged ligand admixtures reducing the Mn amplitudes to 63.5% and to 75.9%, respectively. In the symmetric 28a′ component a mixing between Mn 3 $d_{x^2-y^2}$ and 3 d_{xz} is encountered that leads to a rotation of the Mn 3d orbitals. The in-phase coupling with the Cp moiety is reinforced and the antibonding interaction with the benzene π functions is reduced.

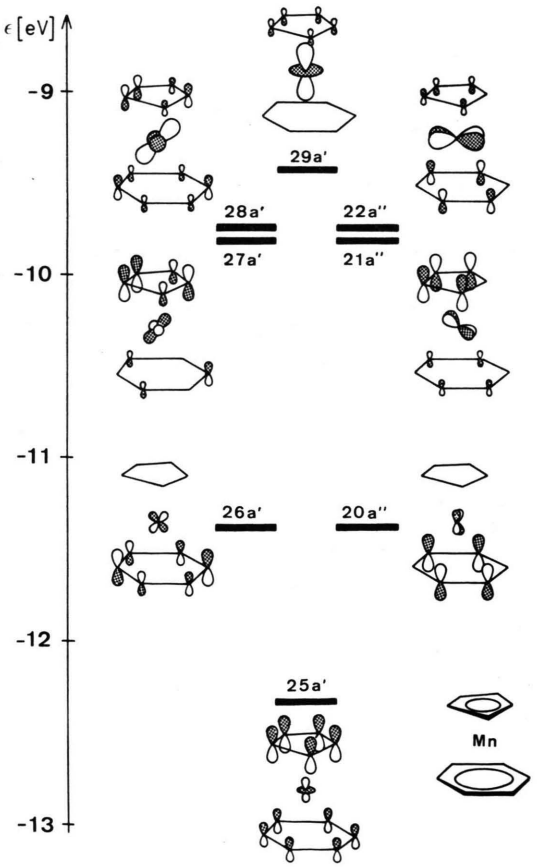

Fig. 1. Schematic representation of the molecular orbitals of cyclopentadienyl benzene manganese **4** in the outer valence region.

Table 3. Wiberg bond indices in the closed shell metallocenes **1**—**4** according to INDO calculations.

Compound	Bond	Bond Index
1	MgC	0.211
	CC	1.320
2	CrC	0.366
	CC	1.276
3	FeC	0.281
	CC	1.304
4	MnC_{Cp}	0.300
	MnC_{Bz}	0.302
	CC_{Cp}	1.307
	CC_{Bz}	1.315

28a′ and 22a″ are nearly degenerate with the ligand e_1 descendants 27a′ and 21a″ that are localized in the fivemembered ring; benzene admixtures are small. The Mn 3d contributions ($3d_{xz}$, $3d_{yz}$, $3d_{x^2-y^2}$ and $3d_{xy}$) in both ligand orbitals lead to an enhanced coupling with the Cp ring (out-of-plane rotation of the Mn 3d basis functions). The next MO pair with an e_1 parent (26a′/20a″) is predicted at −11.47 eV; the two complex orbitals are derived from the $1e_{1g}$ MO of benzene. In comparison to the Cp e_1 descendants a less pronounced metal ligand interaction is diagnosed. Significant π contributions from both organic ligands are found in the 25a′ MO at −12.32 eV. The remaining σ MO's in the interval between −12.99 eV to −13.69 eV are either localized in the fivemembered ring or are located in the benzene fragment.

In order to get some insight into the nature of the metal ligand interaction in the series **1**—**4** we have summarized Wiberg bond indices [46] in Table 3. The covalent coupling between the central atom and the organic π ligands is largest in the Cr complex and is smallest in the Mg sandwich. The iron and manganese compounds are between these two extremes. The CC indices in the sixmembered rings of **2** are smaller than the Wiberg indices in the C_6H_6 ligand of **4**. This must be traced back to the stronger metal-to-ligand charge transfer in the Cr derivative; the surplus of negative charge in **4** is predicted in the Cp moiety.

4. The Vertical Ionization Energies in the Outer Valence Region

The He(I) PE spectrum of **1** has been measured by Evans et al. [13]. Two well resolved peaks with maxima at 8.26 eV and 9.14 eV are detected in the region below 10 eV. In the interval between 12.2—14.0 eV a broad, strongly overlapping band system is found. The band maxima are 13.5 and 12.5 eV, a low energy shoulder at 12.2 eV has also been verified.

The Green's function results for **1** are displayed in Table 4. We have considered 14 hole-states and 10 particle-functions in the perturbational summation of the self-energy part. It is seen that the computational results are close to the measured ionization energies. Ionization potentials of 7.77 and 8.92 eV are calculated for the $4e_{1g}$ and $5e_{1u}$ ionization events. The experimental gap $4e_{1g}/5e_{1u}$ (0.88 eV) has to be compared with the theoretically determined separation of 1.15 eV. Koopmans' defects are smaller than 0.2 eV. The deviations from $I^K_{v,j}$ are enhanced with increasing orbital energies. The defect components generally oscillate between 0.4 eV and 1.4 eV for the $6a_{1g}$ orbital. A decomposition of the total reorganization energy of 1.4 eV into relaxation and correlation contributions shows that the deviations from $I^K_{v,j}$ are due to the variation of the pair correlation in the cationic hole-state (>90%); relaxation effects within the HF picture are negligible [47].

Three bands with maxima at 5.45, 6.46 and 9.80 eV are found in the low energy region of **2** [14—16]. The third peak has a low energy shoulder at 9.56 eV. The following band system between 11 and 13 eV shows maxima at 11.39, 11.90 and 12.70 eV. The integrated band intensities under He(I) and He(II) conditions are in line with the

Table 4. Comparison between measured vertical ionization potentials, $I^{exp}_{v,j}$, of **1** and calculated ones assuming the validity of Koopmans' theorem ($I^K_{v,j}$) and using the inverse Dyson equation with a second order approximation to the self-energy part ($I^K_{v,j} + \Sigma^{(2)}_{jj}(\omega_j)$) and the renormalized model potential ($I^K_{v,j} + \Sigma^{eff}_{jj}(\omega_j)$). All values in eV. (max = maximum, sh = shoulder).

Band	Assignment	$I^K_{v,j}$	$I^K_{v,j} + \Sigma^{(2)}_{jj}(\omega_j)$	$I^K_{v,j} + \Sigma^{eff}_{jj}(\omega_j)$	$I^{exp}_{v,j}$
1	$4e_{1g}$	7.96	7.76	7.77	8.26
2	$5e_{1u}$	9.11	8.91	8.92	9.14
3	$5a_{2u}$	12.41	11.54	11.64	
	$3e_{2u}$	12.32	11.84	11.88	12.2_{sh}
	$4e_{1u}$	12.32	11.93	11.97	12.5_{max}
	$3e_{1g}$	13.06	12.59	12.64	
	$3e_{2g}$	13.10	12.63	12.68	13.5_{max}
	$6a_{1g}$	15.66	14.05	14.22	

following assignment: ① = $8a_{1g}$, ② = $4e_{2g}$, ③ = $4e_{1g}/6e_{1u}$. The intensity ratio for the He(I) source is 1.0 : 4.0 : 9.0, the He(II) intensities amount to 1.0 : 2.0 : 3.2.

The He(I)/He(II) technique allowed also a clear discrimination of the IP sequence in the third maximum. The low energy shoulder at 9.56 eV must be assigned to the $4e_{1g}$ combination with Cr $3d_{xz}/3d_{yz}$ contributions while the band maximum at 9.80 eV has its origin in ionization processes out of $6e_{1u}$. The first IP of **2** as determined by PE spectroscopy differs by about 0.5 eV from the value obtained by mass spectrometry (5.91 eV) [48].

The calculated IP's of **2** are displayed in Table 5; 14 hole- and 10 particle-functions have been taken into account in the self-energy expansion. The sequence of the ionization processes is correctly predicted by the computational procedure. On the other hand deviations in the absolute energies are observed. An ionization energy of 7.13 eV is calculated for the strongly localized $8a_{1g}$ MO. The theoretically determined Koopman's defect is found to be 1.39 eV. In second order of perturbation an $I^{K}_{v,j}$ reduction of 1.61 eV is diagnosed while the renormalization via the D4 increment is −0.22 eV. The reorganization energy for the $4e_{2g}$ MO is only 0.55 eV, an increment that is comparable with Koopmans' defects of ligand ionization processes. The calculated energy difference between $8a_{1g}$ and $4e_{2g}$ (1.43 eV) is close to the experimental gap of about 1 eV. Below we have compared the Green's function (GF) INDO results with ΔSCF ab initio calculations and a transition state approach in the X_α approximation. It is recognized that the ΔSCF results differ significantly form the measured IP's.

Table 5. Comparison between measured and calculated ionization potentials of **2**; see legend Table 4. (sh = shoulder).

Band	Assignment	$I^{K}_{v,j}$	$I^{K}_{v,j}+\Sigma^{(2)}_{jj}(\omega_j)$	$I^{K}_{v,j}+\Sigma^{eff}_{jj}(\omega_j)$	$I^{exp}_{v,j}$
1	$8a_{1g}$	8.52	6.91	7.13	5.45
2	$4e_{2g}$	9.14	8.55	8.59	6.46
3	$4e_{1g}$	11.25	10.73	10.78	9.56_{sh}
	$6e_{1u}$	11.21	10.90	10.91	9.80
4	$6a_{2u}$	11.71	11.38	11.39	11.4
	$3e_{2u}$	12.45	11.99	12.04	11.9
	$3e_{2g}$	12.82	12.23	12.29	12.7

	$I^{exp}_{v,j}$	$I^{GF/INDO}_{v,j}$	$I^{\Delta SCF}_{v,j}$ [14]	$I^{X\alpha}_{v,j}$ [33]
$^2A_{1g}$	5.45	7.13	5.1	6.60
$^2E_{2g}$	6.46	8.59	4.9	7.33

(all values in eV)

The benzene π sequence $4e_{1g}$ on top of $6e_{1u}$ is also reproduced by the theoretical approach. The larger reorganization accompanying the $4e_{1g}$ ionization (0.47 eV) in comparison to $6e_{1u}$ (0.30 eV) leads to a switch of the corresponding ground state ordering. The calculated gap between the two degenerate ligand combinations amounts to 0.13 eV, the experimental separation is 0.24 eV. The remaining calculated ligand π and σ ionization energies (Table 5) are close to the measured IP's.

The PE spectrum of ferrocene **3** has been measured by various groups [13, 17, 18, 49]. The first band at 6.86 eV corresponds to an ionization event out of the $4e_{2g}$ combination, the second maximum at 7.23 eV is very sharp indicating the nonbonding nature of the MO from which the electron has been ejected. This peak has been assigned to the $8a_{1g}$ orbital. The third band in the PE spectrum of **3** has two maxima at 8.8 and 9.3 eV that must be traced back to the two Cp π combinations $6e_{1u}$ and $4e_{1g}$. Evans at al. [17] derived the sequence $6e_{1u}$ on top of $4e_{1g}$ while Rabalais et al. [18] favoured the opposite sequence. The first assignment was in line with a near minimal basis ΔSCF study while double-zeta calculations predicted the latter one [2]. The results of Evans et al. [17] have been corroborated unequivocally by a very recent study under He(I) and He(II) radiation conditions [49]. The remaining IP's of **3** in the lower energy region are found between 11.8 and 14 eV with maxima at 12.3, 13.0 and 13.49 eV and with a weak shoulder (11.9 eV) at the lower energy side.

The computational results for ferrocene are collected in Table 6. 17 hole- and 10 particle-states have been included in the perturbational summation. It is seen that the method fails to predict the sequence of the first two bands. The calculated IP's are 7.79 eV ($8a_{1g}$) < 8.52 eV ($4e_{2g}$). The same defect has been experienced in ΔSCF calculations with another INDO variant [20] and in transition state calculations in the X_α framework [37]. The ionization energies calculated by Rösch and Johnson are close to the perturbational INDO results ($8a_{1g}(X_\alpha) = 7.9$ eV, $4e_{2g}(X_\alpha) = 8.5$ eV). On the

Table 6. Comparison between measured and calculated ionization potentials of **3**; see legend Table 4. (max = maximum, sh = shoulder).

Band	Assignment	$I^K_{v,j}$	$I^K_{v,j}+\Sigma^{(2)}_{jj}(\omega_j)$	$I^K_{v,j}+\Sigma^{eff}_{jj}(\omega_j)$	$I^{exp}_{v,j}$
1	$4e_{2g}$	11.22	7.55	8.52	6.86
2	$8a_{1g}$	10.75	6.63	7.79	7.23
3	$6e_{1u}$	9.91	9.53	9.57	8.8
	$4e_{1g}$	10.94	10.22	10.35	9.3
4	$6a_{2u}$	11.62	10.95	11.03	11.9_{sh}
	$5e_{1u}$	13.37	12.66	12.75	12.3_{max}
	$3e_{1g}$	14.04	13.18	13.31	13.0_{max}
	$3e_{2u}$	14.03	13.27	13.37	
	$3e_{2g}$	14.29	13.37	13.50	13.5_{max}
	$7a_{1g}$	16.17	14.47	14.69	

other hand ΔSCF ab initio models reproduce the experimental findings [2].

The calculated reorganization energies summarized in Table 6 indicate clearly the nonvalidity of Koopmans' theorem in the case of ferrocene. The net defect for the $4e_{2g}$ ionization amounts to 2.70 eV; in second order of perturbation $I^K_{v,j}$ is reduced by 3.67 eV, the renormalization correction is −0.97 eV. Similar increments are encountered in the Fe $3d_{z^2}$ MO ($8a_{1g}$). The second order contribution to the self-energy expansion is 4.12 eV while a net defect of 2.96 eV is predicted. The reorganization energies for most of the remaining ionization processes are less than 1 eV. The large corrections for $4e_{2g}$ and $8a_{1g}$ lead to an IP sequence that differs from the succession of the canonical MO's in the electronic ground state.

The He(I) PE spectrum of the mixed sandwich **4** has been recorded by Evans et al. [16]. Five separate maxima can be discriminated in the outer valence region below 11 eV. Bands ① and ② with a relative intensity ratio of 1 : 3 at 6.36 and 6.72 eV have to be assigned to ejections out of the Mn 3d MO's 29a′, 22a″ and 28a′, respectively. In analogy to **2** the first IP is raised by about 0.6 eV in the case of a mass spectrometric measurement [48, 50]. The following band maxima of **4** (8.75, 9.25 and 9.79 eV) belong to a series of strongly overlapping bands in an interval between 8.5 and 10 eV. The three IP's in this region must be traced back to ionizations out of the ligand π combinations: 27a′, 21a″, 26a′ and 20a″ (e_1 descendants). The intensity of the fifth maximum comes up to the cross sections of peaks ③ and ④. A broad band system is found above 11 eV, the maxima amount to 11.4, 12.2, 13.0 and 13.4 eV.

The Green's function results are given in Table 7 and are graphically displayed in Figure 2. We have employed an array of 17 hole-states and 10 particle-functions. In correspondence with the experiment $^2A_1$ (a_1 descendent) is predicted to be the cationic ground state; experimental (6.36 eV) and theoretically determined (6.48 eV) ionization energies are almost in perfect agreement. The net reorganization of the 29a′ ionization (2.96 eV) is the result of a second order correction of 4.32 eV and a renormalization of −1.36 eV. A larger difference between theory and experiment is observed for the two e_2 descendants 22a″/28a′ (exp: 6.72 eV, cal: 7.72/8.02 eV). The Koopmans' defects are 2.05 and 1.74 eV, respectively. The 27a′/21a″ ionization energies are quantitatively reproduced by means of the Green's function approach (exp.: 8.75/9.25 eV, cal: 8.92/9.25 eV). The degeneracy between 27a′ and 21a″ in the ground state is lifted in the cationic hole-states due to different degrees of electronic reorganization. The ground state degeneracy of 26a′/20a″ is not perturbed in the two hole-states, a result that is in line with the measured PE spectrum. On the other hand the 26a′/20a″ ionization processes are predicted at too high energies. The remaining ligand π and σ ionization potentials are reproduced with high accuracy. The weak

Table 7. Comparison between measured and calculated ionization potentials of **4**; see legend Table 4. (max = maximum).

Band	Assignment	$I^K_{v,j}$	$I^K_{v,j}+\Sigma^{(2)}_{jj}(\omega_j)$	$I^K_{v,j}+\Sigma^{eff}_{jj}(\omega_j)$	$I^{exp}_{v,j}$
1	29a′	9.44	5.12	6.48	6.36
2	22a″	9.77	6.98	7.72	6.72
	28a′	9.77	7.41	8.03	
3	27a′	9.78	8.65	8.92	8.75
4	21a″	9.79	9.10	9.25	9.25
5	26a′	11.47	10.94	11.09	9.79
	20a″	11.47	10.93	11.02	
6	25a′	12.32	11.38	11.54	11.4
	24a′	12.99	12.28	12.39	12.2_{max}
	19a″	13.02	12.30	12.40	
	23a′	13.13	12.45	12.55	
	18a″	13.14	12.45	12.55	13.0_{max}
	22a′	13.58	12.78	12.88	
	17a″	13.69	12.90	13.00	

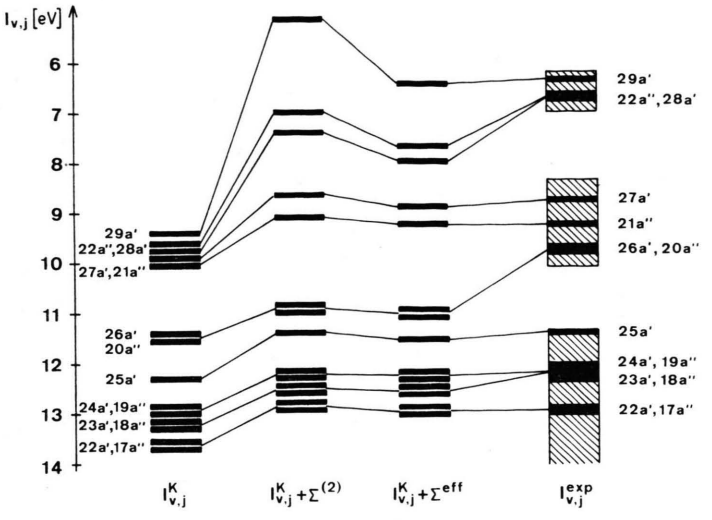

Fig. 2. Comparison between the measured vertical ionization potentials, $I^{exp}_{v,j}$, of **4** and calculated ones assuming the validity of Koopmans' theorem, $I^K_{v,j}$, and using the Green's function approach with a second order self-energy potential ($I^K_{v,j} + \Sigma^{(2)}$) and the renormalized model operator ($I^K_{v,j} + \Sigma^{eff}$).

maximum at 11.4 eV is assigned to the 25a′ combination (ligand π) while the intense component at 12.2 eV should correspond to ejections out of the 24a′, 19a″, 23a′ and 18a″ orbitals. The maximum at 13.0 eV is assigned to the Cp σ MO's 22a′ and 17a″.

5. Conclusion

Outer valence ionization potentials of closed shell metallocenes have been calculated by means of a perturbational expansion based on the Green's function formalism and have been compared with experimental values. The wave functions and one-electron energies for the various calculations were determined by a semiempirical INDO Hamiltonian. It has been shown that only the PE spectrum of the Mg complex **1** without occupied 3d functions can be assigned on the basis of Koopmans' theorem. In the case of the metallocenes **2**—**4** large deviations between $I^K_{v,j}$ and calculated ionization energies under the inclusion of relaxation and correlation have been encountered. With exception of the $4e_{2g}/8a_{1g}$ sequence in ferrocene the experimental findings are reproduced by the Green's function method. Deviations between measured ionization energies and calculated ones must be traced back to the approximative nature of the employed MO model and to the necessary limitations in the allocation of the particle- and hole-arrays in the self-energy expansion.

The calculated Koopmans' defects in the series **2**—**4** are largest for strongly localized metal 3d orbitals of A_1 ($3d_{z2}$) and E_2 ($3d_{x^2-y^2}/3d_{xy}$) symmetry. The reorganization energies for ionization events out of these MO's are summarized in Table 8. It is recognized that the defect components in the Fe and Mn complexes **3** and **4** are similar while the reorganization energies in the Cr derivative **2** are significantly smaller. The net deviations from $I^K_{v,j}$ of the a_1 descendants amount to 1.39 eV in **2** but to about 3 eV in the metallocenes **3** and **4**. The differences between the Cr and the Fe/Mn complexes are even more pronounced in the two e_2 descendants. Comparable Koopmans' defects are calculated for the $8a_{1g}$ and $4e_{2g}$ orbitals in the ferrocene molecule as a result of similar localization properties of the two wave functions. The stronger metal ligand interaction within the e_2 derivatives of the mixed sandwich **4** leads to a reduction of the corresponding reorganization energies. The calculated Koopmans' defects of 1.74 and 2.05 eV are only 2/3 of the a_1

Table 8. Calculated reorganization energies for the strongly localized complex orbitals with predominant 3d amplitudes in the series **2**—**4**; all values in eV.

Compound	Γ_j	$\Sigma^{(2)}_{jj}(\omega_j)$	D4(ε_j)	$\Sigma^{eff}_{jj}(\omega_j)$
2	$8a_{1g}$	1.61	— 0.22	1.39
	$4e_{2g}$	0.59	— 0.04	0.55
3	$8a_{1g}$	4.12	— 1.16	2.96
	$4e_{2g}$	3.67	— 0.97	2.70
4	29a′	4.32	— 1.36	2.96
	28a′	2.36	— 0.62	1.74
	22a″	2.79	— 0.74	2.05

correction. For the $4e_{2g}$ combination of the Cr complex only an $I^{K}_{v,j}$ deviation of 0.55 eV is predicted although the Cr 3d admixtures to the orbital wave function are comparable to the metal character in the e_2 descendants of the mixed sandwich **4**. The perturbational correction is of the same magnitude as for typical ligand π and σ ionization events in the outer valence region.

The divergent behaviour between **2** on one side and **3**/**4** on the other can be rationalized on the basis of (4) which is the second order (diagonal) contribution to the self-energy operator.

$$\Sigma^{(2)}_{jj}(\omega_j) = \tfrac{1}{2}\sum_k \sum_l \sum_a \frac{V^2_{jk[la]}}{\omega_j + \varepsilon_a - \varepsilon_k - \varepsilon_l - i\eta}\, \bar{n}_a n_k n_l + \tfrac{1}{2}\sum_a \sum_b \sum_k \frac{V^2_{ja[bk]}}{\omega_j + \varepsilon_k - \varepsilon_a - \varepsilon_b + i\eta}\, \bar{n}_a \bar{n}_b n_k \,, \quad (4)$$

$$V_{ij[kl]} = V_{ijkl} - V_{ijlk} \,, \quad (5)$$

$$n_k \begin{cases} = 1 \text{ for an occupied spin-orbital in the ground state,} \\ = 0 \text{ for an unoccupied spin-orbital in the ground state,} \end{cases} \quad (6)$$

$$\bar{n}_k = 1 - n_k \,. \quad (7)$$

η in (4) is a small positive number. The ZDO adapted four-index transformation of the V_{ijkl} integrals is given in (8). α and γ symbolize AO basis functions.

$$V_{ijkl} = \sum_\alpha \sum_\gamma c_{i\alpha} c_{j\alpha} c_{k\gamma} c_{l\gamma} \cdot \langle \alpha(1)\,\alpha(1) | (1/r_{12}) | \gamma(2)\,\gamma(2) \rangle + V^{ex} \,. \quad (8)$$

V^{ex} contains the one-center exchange integrals of the INDO approximation and has been defined in [8].

The first sum in (4) contains two hole- and one particle-indices (2h 1p) and exceeds the second (2p 1h) contribution [22]. This component furthermore can be decomposed into relaxation contributions and into the variation of the pair correlation in the cationic hole-state as many-body response to the electronic relaxation. The second sum in (4) takes into account the loss of pair correlation in the N electron system due to the ionization process [51]. The magnitude of the physically feasible increments (relaxation and correlation) of $\Sigma^{(2)}_{jj}(\omega_j)$ in 3d complexes has been investigated in recent contributions [22, 52].

The defect components of the self-energy expansion are determined by the absolute values of the four-index integrals $V_{ij[kl]}$ or V_{ijkl}, respectively on one side and by the various particle- and hole-summations that enter the $\Sigma(\omega)$ expansion on the other side. Recently we have shown that Koopmans' defects in 3d complexes are largest if a comparable number of strongly localized hole- and particle-states are available [53]. This balance between particle- and hole-functions is obviously fulfilled in $d^5 - d^6$ complexes. With increasing d occupation the capability of the virtual MO space with large transition metal amplitudes is reduced while the capability of the occupied Fermi-sea in the scattering events is less efficient for complexes with a smaller number of d electrons.

In a rough model the closed shell metallocenes **2**—**4** can be classified as d^6 complexes; the influence of the particle- and hole-states to the $\Sigma(\omega)$ expansion therefore should be comparable in the three systems and deviations from $I^{K}_{v,j}$ must be traced back to variations in the two-electron integrals $V_{ij[kl]}/V_{ijkl}$. In the first transition metal series diffuse d orbitals are found at the extreme left (Sc, Ti, V) while the 3d AO's at the right (Ni, Cu, Zn) have their probability maxima nearer to the nuclei [54]. This modification in the 3d AO's has two effects on the MO integrals V_{ijkl} that act into the same direction. Diffuse 3d orbitals lead to smaller one-center Coulomb integrals which are the most important terms in the various self-energy numerators [22] and to enlarged metal ligand coupling. Both effects reduce the magnitude of the V_{ijkl} integrals and thus reduce the calculated reorganization energies. We have demonstrated [22, 52] that increasing delocalization of the orbital wave function and enhanced assimilation of the 3d and ligand one-center integrals result in an almost perfect compensation of electronic relaxation and correlation in the $\Sigma(\omega)$ expansion. This condition is obviously fulfilled in the $4e_{2g}$ combination of bis-benzene chromium **2**.

The variation of the V_{ijkl} elements in the series Cr→Mn→Fe allows a straightforward explanation of the different reorganization energies in the Cr complex **2** on one side and the Mn/Fe metallocenes **3**/**4** on the other. The simple model however is insufficient to rationalize the fact that **3** and **4** show comparable Koopmans' defects for the strongly localized MO's although ferrocene has the

larger one-center Coulomb integrals. The 3d elements for Cr, Mn and Fe that are employed in the INDO model are summarized below:

	γ_{3d3d} (eV)
Cr	12.45
Mn	13.72
Fe	14.71

A magnification of the reorganization energies from the Mn complex **4** to the iron derivative **3** should be expected. The relatively large Koopmans' defects of the mixed sandwich **4** can be explained due to the stronger metal ligand coupling between the $3d_{xz}/3d_{yz}$ AO's and ligand π orbitals of proper symmetry. The Mn admixtures in 27a'/21a'' exceed the Fe 3d contributions in $4e_{1g}$. In a previous contribution we have demonstrated that complex orbitals with comparable localization properties in the occupied and empty Fermi-sea are a necessary condition for the accumulation of 2h1p and 2p1h contributions to the self-energy operator [22]. If occupied and virtual orbitals with significant $3d_{xz}/3d_{yz}$ admixtures are neglected in the determination of the self-energy operator the (expected) graduation is calculated, the $I^{K}_{v,j}$ deviations in ferrocene exceed the corrections in the mixed sandwich. The small coupling via $3d_{xz}/3d_{yz}$ in the Cr complex **2** is an additional factor that favours the reduced Koopmans' defects in bisbenzene chromium.

In [53] we have shown that deviations from $I^{K}_{v,j}$ go through a maximum in the 3d series due to the superposition of the V_{ijkl} influence and the potential capability of the particle- and hole-channels as a function of the 3d occupation number. In the d^6 series **2**—**4** we are on the ascend branch of the 3d series, reorganization effects are enhanced with enlarged atomic numbers of the 3d center. In the case of Ni—Zn complexes the V_{ijkl} influence is overcompensated due to the modified number of particle- and hole-states and the deviations from $I^{K}_{v,j}$ are reduced.

It is also possible to extrapolate these theoretical findings from the 3d series to the 4d (Y—Cd) and 5d (La—Hg) series. The covalent metal ligand coupling is strengthened due to the more diffuse valence orbitals; this has been demonstrated in the PE spectra of bis(π-allyl) complexes with Ni, Pd and Pt [55]. The increasing delocalization in 4d and 5d complexes of course leads to a reduction of the V_{ijkl} integrals and thus to a reduction of relaxation and correlation effects. The larger importance of many-body interactions in 3d complexes in comparison to 4d or 5d derivatives has been verified in various MO studies on binuclear transition metal compounds [56—59].

The strong coupling between calculated reorganization energies and the localization properties of the orbital wave function has been verified due to the cross sections for the PE bands under He(I) and He(II) conditions. In the last section it has been mentioned that the intensity of ligand bands exceeds the intensity of transition metal ionization processes for the He(I) source. This relation is modified under He(II) conditions where the metal cross sections are raised. This dependence can be explained on the basis of (9) which is the transition moment for the photoionizing process [60].

$$I \infty |\langle \varphi_j | \sum_n p_n |u_k\rangle \langle a_j \psi_0 | \psi_j^{(N-1)}\rangle|^2 . \qquad (9)$$

The predominant contribution arises from the threefold product $\langle \varphi_j | \sum_n p_n |u_k\rangle$ where φ_j is the wave function of the j'th canonical MO that has lost the electron, p_n is the linear momentum operator and u_k symbolizes the wave function of the ejected electron which is conveniently given in a plane wave approximation (see (10)). $\langle a_j \psi_0 | \psi_j^{(N-1)}\rangle$ is the overlap amplitude between the unrelaxed wave function of the $(N-1)$ electron system and the exact wave function of the j'th hole-state.

$$u_k = N \cdot e^{-ikr} , \qquad (10)$$

N = normalization constant

$$k = [2m(\hbar w - I_j)^{1/2}]\,\hbar , \qquad (11)$$

w = kinetic energy of the free electron.

The plane wave of the free electron has a de Broglie wave length λ (12), which is of molecular dimensions.

$$\lambda = 12.3\,|\sqrt{\hbar w - I_j} , \qquad (12)$$

λ in Å, w in eV .

The band intensity is largest if the half-width of the j'th MO is approximately of the same dimensions as a quarter of the wave length of the photoelectron [61]. In the case of a delocalized MO the interference between λ and u_k is more efficient under He(I) conditions with the longer wave length of the ejected electron. In the limit of strongly localized orbital wave functions the photoionizing radiation

is enlarged under He(II) conditions. The short wave length radiation now has a better overlap with the "metal MO". As long as variations in the available number of particle- and hole-states can be neglected (isoelectronic systems or isovalenceelectronic molecules) there should be a strong correspondence between theoretically determined reorganization energies and intensity changes under He(I) and He(II) conditions. In the case of the Cr complex **2** and ferrocene **3** this correspondence indeed is encountered. The Koopmans' defects of **2** are significantly smaller than the reorganization energies in **3**. The same graduation has been diagnosed in the PE spectra of **2** and **3** under He(I)/He(II) conditions [15, 49]; the variation of the 3d cross sections in **2** are less pronounced than in **3**.

Acknowledgement

This work has been supported by the Stiftung Volkswagenwerk.

[1] T. Koopmans, Physica **1**, 104 (1934).
[2] M.-M. Coutiere, J. Demuynck, and A. Veillard, Theor. Chim. Acta **27**, 281 (1972); P. S. Bagus, U. I. Wahlgren and J. Almlöf, J. Chem. Phys. **64**, 2324 (1976).
[3] M.-M. Rohmer and A. Veillard, J.C.S. Chem. Commun. 250 (1973); M.-M. Rohmer, J. Demuynck, and A. Veillard, Theor. Chim. Acta **36**, 93 (1974).
[4] J. A. Connor, L. M. R. Derrick, M. B. Hall, I. H. Hillier, M. F. Guest, R. B. Higginson, and D. R. Lloyd, Mol. Phys. **28**, 1193 (1974); M. B. Hall, I. H. Hillier, J. A. Connor, M. F. Guest, and D. R. Lloyd, Mol. Phys. **30**, 839 (1975); J. A. Connor, L. M. R. Derrick, I. H. Hillier, M. F. Guest, and D. R. Lloyd, Mol. Phys. **31**, 23 (1976).
[5] S. Evans, M. F. Guest, I. H. Hillier, and A. F. Orchard, J.C.S. Faraday II **69**, 417 (1973); M. F. Guest, B. R. Higginson, D. R. Lloyd, and I. H. Hillier, J. C. S. Faraday II **71**, 902 (1975).
[6] W. v. Niessen and L. S. Cederbaum, Mol. Phys. **43**, 897 (1981).
[7] D. Saddai, H.-J. Freund, and G. Hohlneicher, Surface Sci. **95**, 527 (1980); D. Saddai, H.-J. Freund, and G. Hohlneicher, Chem. Phys. **55**, 339 (1981).
[8] M. C. Böhm and R. Gleiter, Theor. Chim. Acta **57**, 315 (1981).
[9] M. C. Böhm and R. Gleiter, Chem. Phys. **64**, 183 (1982); M. C. Böhm, M. Eckert-Maksic, R. D. Ernst, D. R. Wilson, and R. Gleiter, J. Amer. Chem. Soc. **104**, 2699 (1982).
[10] M. C. Böhm, Z. Naturforsch. **36a**, 1361 (1981); M. C. Böhm, Z. Phys. Chem. Neue Folge **129**, 149 (1982). Böhm, J. Mol. Struct. (Theochem.) **89**, 165 (1982).
[11] M. C. Böhm, Inorg. Chem. in press.
[12] M. C. Böhm and R. Gleiter, Theor. Chim. Acta **59**, 127, 153 (1981).
[13] S. Evans, M. L. H. Green, B. Jewitt A. F. Orchard, and C. F. Pygall, J. C. S. Faraday II **68**, 1847 (1972).
[14] D. W. Turner, C. Baker, A. D. Baker, and C. R. Brundle, Molecular Photoelectron Spectroscopy, Wiley, New York 1970.
[15] M. F. Guest, I. H. Hillier, R. B. Higginson, and D. R. Lloyd, Mol. Phys. **29**, 113 (1975).
[16] S. Evans, J. C. Green, and S. E. Jackson, J. C.S. Faraday II **68**, 249 (1972).
[17] S. Evans, A. F. Orchard, and D. W. Turner, Int. J. Mass. Spectr. Ion Physics **7**, 261 (1971).
[18] J. W. Rabalais, L. O. Werme, T. Bergmark, L. Karlson, M. Hussain, and K. Siegbahn, J. Chem. Phys. **57**, 1185 (1972).
[19] R. F. Kirchner, G. H. Loew, and U. T. Mueller-Westerhoff, Theor. Chim. Acta **41**, 1 (1976).
[20] M. C. Zerner, G. H. Loew, R. F. Kirchner, and U. T. Mueller-Westerhoff, J. Amer. Chem. Soc. **102**, 589 (1980).
[21] M. C. Böhm, Ber. Bunsenges. Phys. Chem. **86**, 56 (1982).
[22] M. C. Böhm, Chem. Phys. **67**, 255 (1982); M. C. Böhm, Int. J. Quantum Chem. in press.
[23] F. Ecker and G. Hohlneicher, Theor. Chim. Acta **25**, 289 (1972); P. O. Nerbrant, Int. J. Quantum Chem. **9**, 901 (1975).
[24] L. S. Cederbaum and W. Domcke, Adv. Chem. Phys. **36**, 205 (1977); W. v. Niessen, L. S. Cederbaum, W. Domcke, and J. Schirmer, Computational Methods in Chemistry, ed. J. Bargon, Plenum Press, New York 1980.
[25] L. S. Cederbaum, Theor. Chim. Acta **31**, 239 (1973); L. S. Cederbaum, J. Phys. B **8**, 290 (1975).
[26] F. J. Dyson, Phys. Rev. **75**, 486 (1949).
[27] D. S. Marynick, J. Amer. Chem. Soc. **99**, 1436 (1977); M. J. S. Dewar and H. S. Szepa, J. Amer. Chem. Soc. **100**, 777 (1978).
[28] N. S. Chiu and L. Schaefer, J. Amer. Chem. Soc. **100**, 2604 (1978); E. D. Jemmis, S. Alexandratos, P. v. R. Schleyer, A. Streitwieser, and H. F. Schaefer III, J. Amer. Chem. Soc. **100**, 5695 (1978); J. Demuynck and M.-M. Rohmer, Chem. Phys. Letters **54**, 567 (1978); R. Gleiter, M. C. Böhm, A. Haaland, R. Johansen, and J. Lusztyk, J. Organomet. Chem. **170**, 285 (1979).
[29] A. Almenningen, O. Bastiansen, and A. Haaland, J. Chem. Phys. **40**, 3424 (1964); C. Wong, T. Y. Lee, K. J. Chao, and S. Lee, Acta Cryst. **B28**, 1662 (1972); C. Wong, T. Y. Lee, T. W. Chang, and C. S. Lin, Inorg. Nucl. Chem. Lett. **9**, 667 (1979); A. Almenningen, A. Haaland, and J. Lusztyk, J. Organomet. Chem. **170**, 271 (1979).
[30] A. Haaland, J. Lusztyk, D. P. Novak, J. Brunvoll, and K. B. Starowieyski, J. C. S. Chem. Commun. 1974, 54.
[31] E. M. Shustorovich and M. E. Dyatkina, Dokl. Akad. Nauk. SSSR **128**, 1234 (1959); I. H. Hillier and R. M. Canadine, Discuss. Faraday Soc. **47**, 27 (1969); S. E. Anderson and R. S. Drago, Inorg. Chem. **11**, 1564 (1972).
[32] J. Y. Saillard, D. Grandjean, F. Choplin, and G. Kaufman, J. Molec. Struct. **23**, 363 (1974); N. J. Fitzpatrick, J. M. Savariault, and J. F. R. Labarre, J. Organomet. Chem. **127**, 325 (1977).
[33] J. Weber, M. Geoffroy, A. Goursot, and E. Pénigault, J. Amer. Chem. Soc. **100**, 325 (1977).
[34] F. A. Cotton, W. A. Dollase, and J. S. Wood, J. Amer. Chem. Soc. **85**, 1543 (1963); F. Jellinek, J. Organomet. Chem. **1**, 43 (1963).

[35] R. Hoffmann, A. Imamura, and W. J. Hehre, J. Amer. Chem. Soc. **90**, 1499 (1968); R. Hoffmann, Acc. Chem. Res. **4**, 1 (1971); R. Gleiter, Angew. Chem. **86**, 770 (1973).
[36] E. M. Shustorovich and M. E. Dyatkina, Zh. Strukt. Khim. **1**, 98 (1960); J. P. Dahl and C. J. Ballhausen, K. Dan. Vidensk. Selek., Mat.-Fys. Medd. **33**, 5 (1961); R. D. Fischer, Theor. Chim. Acta **1**, 418 (1963); J. H. Schachtschneider, R. Prins, and P. Ros, Inorg. Chim. Acta **1**, 462 (1967); A. T. Armstrong, D. G. Caroll, and S. P. McGlynn, J. Chem. Phys. **47**, 1104 (1967); A. Botrel, P. Dibout, and R. Lissillour, Theor. Chim. Acta **37**, 37 (1975).
[37] E. J. Baerends and P. Ros, Chem. Phys. Letters **23**, 391 (1973); N. Rösch and K. H. Johnson, Chem. Phys. Letters **24**, 179 (1974).
[38] J. H. Ammeter, H.-B. Bürgi, J. C. Thibeault, and R. Hoffmann, J. Amer. Chem. Soc. **100**, 3686 (1978).
[39] R. K. Bohn and A. Haaland, J. Organomet. Chem. **5**, 470 (1966); P. Seiler and J. D. Dunitz, Acta Cryst. **B35**, 1068 (1979).
[40] D. W. Clack and K. D. Warren, Struct. Bonding, Vol. **39**, Springer-Verlag, Berlin 1980.
[41] D. W. Clack and K. D. Warren, Theor. Chim. Acta **46**, 313 (1977); D. W. Clack and K. D. Warren, Inorg. Chim. Acta **24**, 35 (1977); D. W. Clack and K. D. Warren, Inorg. Chim. Acta **30**, 251 (1978).
[42] D. W. Clack and K. D. Warren, J. Organomet. Chem. **149**, 401 (1978); D. W. Clack and K. D. Warren, J. Organomet. Chem. **152**, C60 (1978); D. W. Clack and K. D. Warren, J. Organomet. Chem. **157**, 421 (1978).
[43] M. C. Böhm, Chem. Phys. Letters **83**, 533 (1981).
[44] A. F. Berndt and R. E. Marsh, Acta Cryst. **16**, 118 (1963); M. R. Churchill and P. H. Bird, Inorg. Chem. **7**, 1793 (1968); R. M. Kirchner, J. T. Marks, J. S. Kristoff, and J. A. Ibers, J. Amer. Chem. Soc. **95**, 6602 (1973).
[45] K. D. Warren, J. Phys. Chem. **77**, 1681 (1973); K. D. Warren, Struct. Bonding, Vol. **27**, Springer-Verlag, Berlin 1976.
[46] K. B. Wiberg, Tetrahedron **24**, 1083 (1968).
[47] M. C. Böhm, unpublished results.
[48] J. Müller and P. Göser, J. Organomet. Chem. **12**, 163 (1968).
[49] C. Cauletti, J. C. Green, M. R. Kelly, P. Powell, J. v. Tilborg, J. Robbins, and J. Smart, J. Electron Spectrosc. **19**, 327 (1980).
[50] R. G. Denning and R. A. D. Wentworth, J. Amer. Chem. Soc. 88, 4619 (1966).
[51] B. T. Pickup and O. Goscinski, Mol. Phys. **26**, 1013 (1973); G. Born, H. A. Kurtz, and Y. Öhrn, J. Chem. Phys. **68**, 74 (1978).
[52] M. C. Böhm, Theor. Chim. Acta in press.
[53] M. C. Böhm and R. Gleiter, J. Comput. Chem. **3**, 140 (1982).
[54] J. S. Griffith, The Theory of Transition-Metal Ions, Cambridge University Press, Cambridge (1971); M. Gerloch and R. C. Slade, Ligand-Field Parameters, Cambridge University Press, Cambridge 1973.
[55] M. C. Böhm, R. Gleiter, and C. D. Batich, Helv. Chim. Acta **63**, 990 (1980).
[56] M. Benard, J. Chem. Phys. **71**, 2546 (1979).
[57] F. A. Cotton, Acc. Chem. Res. **11**, 225 (1978); F. A. Cotton, Pure Appl. Chem. **52**, 2331 (1980).
[58] P. C. de Mello, W. D. Edwards, and M. C. Zerner, J. Amer. Chem. Soc. **104**, 1440 (1982).
[59] M. M. Goodgame and W. A. Goddard, J. Chem. Phys. **85**, 215 (1981); P. M. Atha and I. H. Hillier, Mol. Phys. **45**, 285 (1982).
[60] L. L. Lohr, Jr., Electron Spectroscopy, ed. D. E. Shirley, North-Holland, Amsterdam 1972; F. O. Ellison, J. Chem. Phys. **61**, 507 (1974).
[61] W. C. Price, A. W. Potts, and D. G. Streets, Electron Spectroscopy, ed. D. E. Shirley, North-Holland, Amsterdam 1972.